Received June 17, 2021, accepted July 14, 2021, date of publication July 20, 2021, date of current version July 27, 2021.
Digital Object Identifier 10.1109/ACCESS.2021.3098532

Recognition of Endemic Bird Species Using Deep Learning Models

YO-PING HUANG[1,2,3,4], (Fellow, IEEE), AND HAOBIJAM BASANTA[1]
[1]Department of Electrical Engineering, National Taipei University of Technology, Taipei 10608, Taiwan
[2]Department of Electrical Engineering, National Penghu University of Science and Technology, Penghu 880011, Taiwan
[3]Department of Computer Science and Information Engineering, National Taipei University, New Taipei City 23741, Taiwan
[4]Department of Information and Communication Engineering, Chaoyang University of Technology, Taichung 41349, Taiwan

Corresponding author: Yo-Ping Huang (yphuang@ntut.edu.tw)

This work was supported in part by the Ministry of Science and Technology, Taiwan, under Grant MOST108-2221-E-027-111-MY3 and Grant MOST109-2622-E-027-001-CC3, and in part by the National Taipei University of Technology International Joint Research Project, under Grant NTUT-IJRP-109-03 and Grant NTUT-IJRP-110-01.

ABSTRACT Numerous bird species have become extinct because of anthropogenic activities and climate change. The destruction of habitats at a rapid pace is a significant threat to biodiversity worldwide. Thus, monitoring the distribution of species and identifying the elements that make up the biodiversity of a region are essential for designing conservation stratagems. However, identifying bird species from images is a complicated and tedious task owing to interclass similarities and fine-grained features. To overcome this, in this study, we developed a transfer learning-based method using Inception-ResNet-v2 to detect and classify bird species endemic to Taiwan and to distinguish them from other object domains. Furthermore, to validate the reliability of the model, we adopted a technique that involves swapping misclassified data between training and validation datasets. The swapped data are retrained until the most suitable result is obtained. Additionally, fivefold cross-validation was performed to verify the predictive performance of the model. The proposed model was tested using 760 images of birds belonging to 29 species that are endemic to Taiwan; the images were captured from various environments with different perspectives and occlusions. Our model achieved an accuracy of 98.39% in the classification of the bird species and 100% in the detection of birds among different object categories. Moreover, the model achieved a precision, recall, and F1-score of 98.49%, 97.50%, and 97.90%, respectively, in classifying bird species endemic to Taiwan.

INDEX TERMS Endemic birds, inception-ResNet-v2, transfer learning, bird classification.

I. INTRODUCTION

The inherent heterogeneity of diverse species in a geographic region is essential for ensuring the stability of an ecosystem. However, the biodiversity of natural habitats has been declining continuously over time [1]. The unnatural destruction of habitats [2] may occur due to natural or unnatural threats [3]–[6], including changes in the food web, habitat fragmentation, resource depletion, nutrient scarcity, climatic shifts, alien species intrusion, all of which are adverse impacts on natural biota of an ecosystem. Every species within a habitat plays an important role in sustaining it. Along with other native organisms, birds play a crucial role in balancing an ecosystem. They are considered keystone species that help maintain sustainable population levels between all living things in the overall web of life [7]. Even a slight decrease in their number endangers the entire ecosystem [8]. Birds occupy many levels of trophic webs; they are mid-level consumers as well as top predators [9]. They bring plants back to ecosystems through pollination or seed dispersal across the sea to new land masses. Many birds are scavengers [10] and they help in the quick disposal of carcasses and in the recycling of nutrients in the ecosystem to maintain a healthy habitat [11]. However, deviations in avian distribution [12] are often the first sign of environmental disturbance, and according to a survey by BirdLife International [13], many bird populations are currently declining worldwide. One in eight bird species is considered to be on the brink of extinction, with 222 species critically endangered with a serious possibility of imminent extinction [14]. Thus, a quick and

The associate editor coordinating the review of this manuscript and approving it for publication was Okyay Kaynak.

effective approach to identify the elements that constitute the biodiversity of a region and monitor their changes over time is necessary for conservation [15].

In this study, we aimed to identify birds that are endemic to Taiwan. Taiwan is located at the intersection of East and Southeast Asia and at a central point along the East Asia–Australasia Flyway (EAAF) [16] large number of avian species that exhibit migratory and vagrant behavior traverse the EAAF. Taiwan spans latitudes of 120° to 122°27′ E and 22° to 25°18′ N. The island consists of shallow coastal waters and steep mountains with a maximum elevation of 3,952 m (12,966 ft); the geography can be roughly categorized as a flat western plain and a rugged mountain range down the spine of the island. In addition, the climate of Taiwan varies considerably; the climate varies from tropical in the south to subtropical in the north, with alpine regions in the mountains. The island experiences abundant rainfall, with an annual average precipitation of 2,510 mm that supports diverse species and biodiversity hotspots of flora and fauna, including 61 mammal species, more than 600 avian species, 37 species of amphibians, 220 species of freshwater fish, 92 species of reptiles, 50,000 species of insects, and more than 400 species of butterfly [17].

Recently, species richness and avian distributions in Taiwan have increased, as observed by both amateurs and professionals. According to the 6th edition of The Clements Checklist of Birds of the World [18], approximately 560 bird species have been identified in Taiwan, with 15 of them endemic to Taiwan. Furthermore, the Chinese Wild Bird Federation (CWBF) checklist, which is updated every three years, indicated that more than 570 bird species have been found throughout Taiwan (2010 CWBF), of which at least 17 species are endemic to Taiwan. In the 2014 CWBF avian checklist report, 626 bird species were recounted, of which 25 were recognized as endemic species and 58 as endemic subspecies. In 2017, the CWBF bird checklist included 653 bird species and recognized 27 endemic species and 56 endemic subspecies. In the latest checklist in 2020, the CWBF recognized 674 bird species, of which 29 were confirmed to be endemic species and 55 were confirmed to be endemic subspecies. Globally, 20% of bird species migrate annually, typically following EAAF migratory routes [19]. According to a recent survey conducted by the Raptor Research Group of Taiwan, several thousand Chinese sparrow hawks migrated over the Hengchun Peninsula in southern Taiwan. In 2020, the survey recorded that 258,132 raptors migrated, breaking the previous record of 257,700 in 2019. Although global bird migration [20] is one of the most common responses to seasonally varying climates, significant changes in the population of invasive alien species may affect natural habitats. Over time, this habitat alteration of ecoregions may result in avifauna becoming endangered and eventually extinct.

Thus, efforts to identify and conserve environments with endemic species should be prioritized to maintain genetic diversity. To improve modelling performance and the knowledge acquired therefrom, in this study, we adopted a transfer learning technique. Moreover, to maintain an efficient ensemble model for each type of species, we adopted the following procedures:

1. We investigated various backbone models of different deep learning architectures, such as Inception-ResNet-v2, InceptionV3, Xception, ResNet101, ResNet101, and MobileNetV2, to achieve efficient feature selection of birds. Then, the performance of all models was evaluated by comparing their accuracies in identifying and classifying bird species when using validation and test data.
2. We chose Inception-ResNet-v2 as the deep learning model because it outperforms other backbone models to a large extent.
3. Furthermore, to enhance the performance and decrease overfitting in the selected model, we proposed a mechanism to swap the training and validation misclassified datasets. Then, we retrained the model until it yielded the highest accuracy possible on the validation and test datasets. Additionally, five-fold cross-validation was employed to verify the predictive performance of the model.

Thus, through the monitoring and identification of endemic birds in their habitats and estimating the size of their populations, the proposed system can help conserve biodiversity.

The structure of this paper is organized as follows. Section II describes data acquisition and preprocessing of acquired dataset to overcome imbalanced and data overfitting. Section III focuses on the deep learning models and enhancement of fine grained feature extraction accuracy by swapping the misclassified data between the training and validation datasets. Section IV illustrates the experimental setting and the hardware requirements. Section V endorses the proof of concept and validation of the purposed methodology. Section VI emphasizes the significances of endemic birds and its habitation. Finally, Section VII summarizes the impact of the purposed model and presents directions for future study.

II. DATA ACQUISITION AND AUGMENTATION

In this study, we upgraded the dataset used in our prior work [21]. Datasets were collected from several online resources. Although Internet images add diversity to the dataset, public domain images may contain noise, spurious pixels, artifacts, and surface roughness; moreover, they may be blurry or distorted. To overcome such problems and limit the deterioration in intensity on the images, the collected images were retained with an average resolution between 1,024 × 768 to 3,008 × 2,000 pixels. Overall, we collected 3,892 images for 29 endemic bird species (Fig. 1).

In deep learning approaches, an algorithm is systematically managed with a multilayered neural network in which a large number of training samples are convolved within several hidden layers between the input and output layers by learning the most complex features to increase its capabilities in

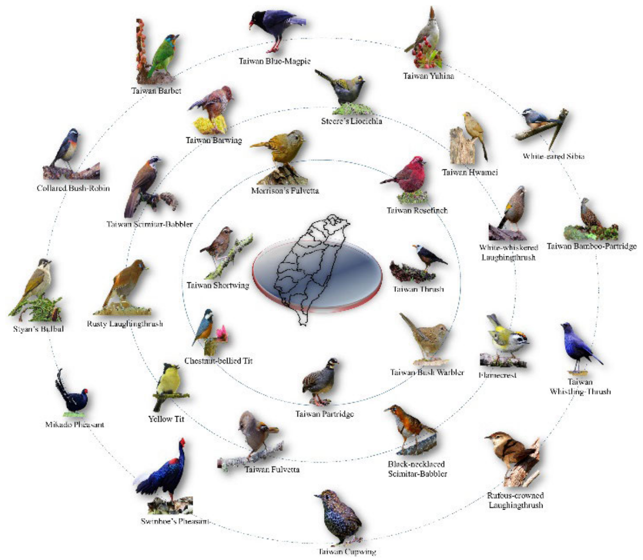

FIGURE 1. Twenty-nine endemic bird species to Taiwan.

predicting or classifying sophisticated data. However, scarce data and constrained resources may cause overfitting, and significant data feature points can be easily missed, affecting the classification accuracy. To counter overfitting and manage the data imbalance, we adopted various types of data augmentation techniques for the images of different bird species based on image feature availability. Images of each species were augmented 10 times, including the original bird images, by using the augmentation techniques such as rotation 45°, Gaussian noise, horizontal/vertical flipping, contrast enhancement, sharpening of images, zoom range [0.7,1.3] and affine transformations.

III. METHODOLOGY

A. TRANSFER LEARNING OF ENDEMIC BIRDS

In recent years, the use of computer vision to overcome the conventional learning paradigm that is designed to solve specific tasks has gained momentum. Conventional learning lacks the inherent ability to transfer knowledge across tasks [22]. Models must be rebuilt from scratch with massive amounts of data to map the changes in the distribution of relevant features. To deal with the scarcity of data and the massive change in data in different homogeneous or heterogeneous target datasets [23], we adopted transfer learning [24]. Transfer learning is usually employed when the new task dataset is smaller than the original dataset. In transfer learning, the algorithm allows for the use of knowledge gained from previously learned tasks and applies it to solve new or similar problems quickly and efficiently. It can determine the subset of relevant complex dimensional feature representations even when only a few labeled datasets are available for training. For instance, in the 2017 CWBF checklist of the birds of Taiwan, 27 endemic bird species were identified, whereas in the 2020 CWBF checklist, 29 endemic bird species were identified. In such a scenario, the knowledge acquired while learning the 27 endemic bird species should be used to solve related tasks pertaining to the 29 endemic bird species. Otherwise, considerable time would be spent every time a new dataset of birds is used. Therefore, to implement the entire process, we adopted a deep-learning-based model (Inception-ResNet-v2) to train and learn the features of 27 endemic bird species (source domain). Then, the learned features were transferred to a second target network to train the newly added dataset on endemic bird species (target domain). Thus, the problem was defined as follows: for a given source domain D_S and learning task L_T and target domain D_T and learning task T_L, the transfer learning technique helps improve the learning of the target predictive function $f_T(\cdot)$ in D_T using the knowledge acquired from D_S and L_T, where $D_S \neq D_T$ *or* $L_T \neq T_L$ [25], [26]. Transfer learning method enables to utilize knowledge from previously learned tasks model A and generalize this knowledge such as features and weights for model B. The transfer learning method for endemic birds is shown in Fig. 2.

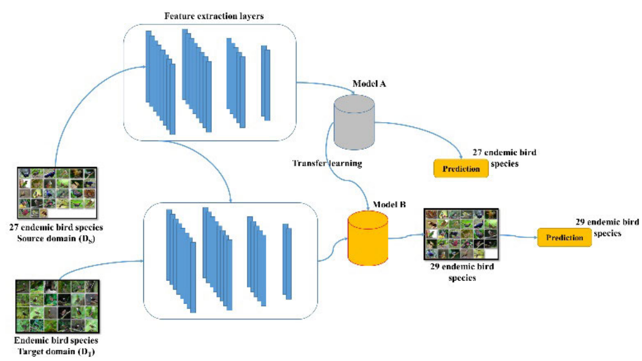

FIGURE 2. Endemic bird species classification using transfer learning module.

B. INCEPTION-RESNET-V2 ARCHITECTURE

In this study, we used Inception-ResNet-v2 [27], which is a hybrid convolutional neural network (CNN) architecture of Inception [28] and a residual network connection [29]. These modules were incorporated with different configuration parameters that make use of the Inception approach by internally attached residual connections with the entire Inception part of the module by replacing the filter concatenation stage of the Inception architecture. Fig. 3 presents a schematic for fine tuning the Inception-ResNet-v2 architecture with different inception modules stacked with a convolutional layer, activation layer, and pooling layer.

In deep learning, a deep network [30], [31] is considered better than a shallow network because it learns relevant features layer-by-layer with more precision and achieves high-level feature extraction (texture, shape, size, color), connecting a set of features to a label from a given set of input categories. However, in practice, deep learning networks have some problems. For instance, deep neural networks often suffer from the problem of vanishing gradients, wherein a deep multilayer feed-forward network is difficult to train and

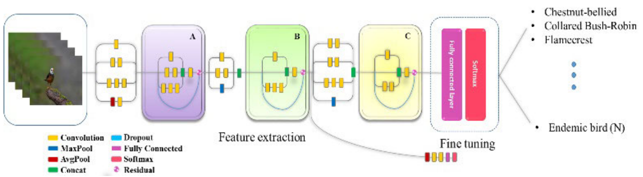

FIGURE 3. **Fine tuning architecture of Inception-ResNet-v2 for classification of endemic birds.**

the parameters of the earlier layers in the network are difficult to tune. Thus, the gradient information from the error function decreases exponentially as the error signals propagate back to an earlier layer. Essentially, when the error signals propagate back to earlier layers, they decrease considerably in magnitude such that the network cannot be learned properly, resulting in premature convergence to an incorrect solution. This problem of degradation in a deep structure is overcome with the use of residual layers in which the input of a CNN layer bypasses one or more layers and adds to the outputs of the stacked layers by learning the residual mappings. Each unit can be expressed as:

$$y_l = h(x_l) + F(x_l, W_l) \tag{1}$$

$$x_{l+1} = f(y_l) \tag{2}$$

where y_l is the residual unit, and x_l and x_{l+1} indicate the input and the output vectors of the l^{th} unit, respectively. The term h is the identity mapping function, F represents the residual function, $W_l = W_{l,S|1 \leq S \leq N}$ is the set of weights of the l^{th} residual unit, S indicates the number of layers in the residual unit, and f is the ReLU activation function. The main logic behind the ResNet is to learn the additive residual function f with respect to $h(x_l)$. An identity mapping function $h(x_l) = x_l$ is used to allow the network to perform well. This is done by adding a shortcut connection that allows the network to train much deeper and easier by eliminating the degradation issues. Thus, integrating the structure of residual connections simplifies Inception considerably by connecting multilayers through a shortcut. This also allows the model to speed up training with deeper neural networks and thereby improve the utilization of resources within the network, which eventually helps prevent the problem of vanishing gradients.

The interior of the Inception-ResNet-v2 network model includes three types of inception modules—Inception-ResNet-A, Inception-ResNet-B, and Inception-ResNet-C blocks—that use 35 × 35, 17 × 7, and 8 × 8 grid modules, respectively, to generate discriminatory features and reduce the number of parameters. To obtain different feature extraction patterns of the bird images, the input size of the images is 299 × 299 pixels with three different color channels (red, green, and blue) for the stem layer. Then, the inception module uses a block of parallel convolutional layers with a multilevel feature extractor that extracts local and generic features from the input images of the birds by computing three different sizes of filters (1 × 1, 3 × 3, and 5 × 5) and a max pooling layer within the same module of the network. The inception module layers use a stride of 1 and the same padding. The outputs of these filters are concatenated along the channel dimension and sent to the next inception module.

Due to the limited numbers of newly found endemic birds, instead of retraining the architectures from scratch fine-tuning of the model is adopted. The final layer of the network is frozen using the previous pretrained weight of 27 endemic birds [21] and obtained the features before classification. Lastly, we feed the concatenated feature vector to the fully connected layer that uses a feature map matrix and weights of inputs to predict the correct label of the bird. Finally, an activation function, softmax, classifies the 29 endemic birds.

C. MULTISTAGE MODEL VALIDATION

The aim of this work was to incorporate a strong backbone network architecture of transfer learning that can facilitate the learning and transfer diverse domain-invariant features from different datasets to a unified feature space to classify endemic bird images of new datasets with high classification accuracy. The deep learning method is systematically managed with a multilayered neural network (NN) in which the layers are densely interconnected. To select the best model hyperparameter, a large dataset is required. The collected data are split into two sets: a training set and test set. Typically, the test set is a holdout dataset used to evaluate how well the model has been trained, indicating the importance of the input value. Then, from the training dataset, T% of the dataset is set as the training set and the rest of the dataset (100 − T)% is set as the validation set, where T is a fixed number (say 70 or 80). The model is then iteratively trained and validated on these different sets. The training set is used to fit the parameters of the classifier, whereas the validation set provides an unbiased evaluation of the model fit on the training set while tuning model hyperparameters, such as the network layer size, finding the optimal number of hidden units, and regularizing the model. Models with few hyperparameters are easy to validate and tune, but if the model has many hyperparameters, a larger validation dataset is required. In some cases, the evaluation is biased when a validation dataset is not incorporated into the model configuration because the model may perfectly fit the training data with high accuracy but may fail to fit the test or validation data. In such cases, k-fold cross-validation, which is a resampling technique, is used to avoid overfitting; the training set is generated with different combinations of k groups (say 5 or 10, depending on the size of the dataset) as the training and validation sets. Then, the model is fit by using (k − 1) folds and evaluated using the remaining k^{th} fold. The process is repeated until every k-fold is used as the test set. However, this may produce varying results. Thus, to improve the model and analyze the influence of various components in the framework, we adopted multistage training with the training and validation datasets (Fig. 4) to better predict test dataset.

The following procedures are used in the approach developed in this study.

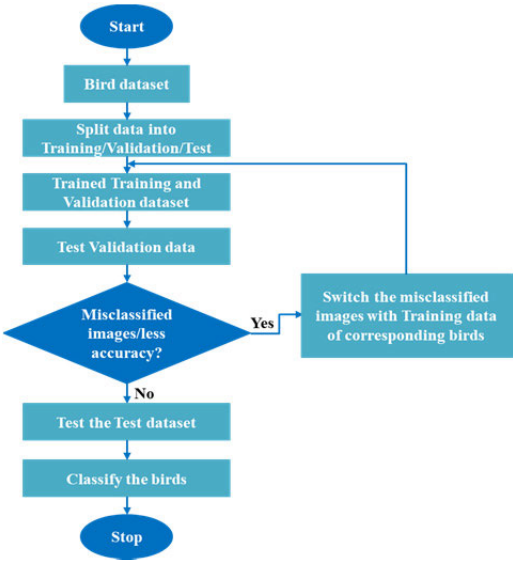

FIGURE 4. Flowchart for model validation.

- Train the Inception-ResNet-v2 architecture on data augmented from original images.
- Test the validation dataset and determine the misclassified images.
- Randomly interchange the same amount of misclassified validation images with the training images and retrain the model again.
- Repeat this process until the classifier adapts to the specific target task.
- Fit the model to evaluate the test set.

In this way, the algorithm can tune itself and improve the generalizability of spatial features to the previously unseen domains present in the image.

IV. EXPERIMENTAL SETTINGS

To extract the relevant features of birds, we randomly split the endemic bird data into 3,132 images for training and 760 images for testing. To allow the deep networks to converge and improve the ability of the model to generalize adeptly, we augmented the training dataset 10 times, resulting in a total of 31,320 images. Then, 25,056 (80%) images were used for training and 6,264 (20%) were used for validation. The Inception-ResNet-v2 model was trained using the mini-batch gradient descent algorithm with the batch size set to 32 and the learning rate maintained at 0.0001. The Adam optimizer was used to fine-tune the model with the following parameters:

- Exponential decay rate of first-moment estimation of 0.9.
- Exponential decay rate of second-moment estimation of 0.999, and a positive scalar value for epsilon of 1e-08.

Furthermore, to avoid overfitting, fivefold cross-validation and early stopping were employed for efficient hyperparameter optimization. The early stopping criterion was based on the model performance when the model stops improving on the holdout validation dataset. The presented work was implemented using the TensorFlow libraries on a GPU workstation with an Intel Xeon 8 CPU, 32 GB of memory, and an Nvidia GeForce 11 GB GRX 2080 Ti graphics card.

V. PROOF OF CONCEPT

In this experiment, 760 images, which were excluded from the training and validation datasets, were used for testing.

A. ACCURACY COMPARISONS OF BENCHMARK NETWORK MODELS

Several experiments were conducted to evaluate the accuracy and practicability of the proposed method. For the quantitative analysis of the models, we first compared state-of-the-art deep learning backbone models, such as Inception-ResNet-v2 [27], Inception-v3 [28], Xception [32], ResNet101 [29], and MobileNetV2 [33]. Fig. 5 lists the classification accuracies achieved by the learning models.

Inception-ResNet-v2 was found to consistently outperform the other existing learning networks by attaining 100% training accuracy, 97.47% validation accuracy, and 97.11% test accuracy.

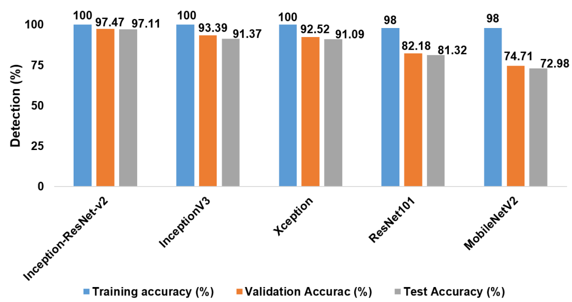

FIGURE 5. Comparison performance of various AI models.

B. ACCURACY OF MULTISTAGE MODEL VALIDATION

To achieve robust and high performance in detecting subtle differences between categories of birds, we adopted two multistage models for validation. One is the Inception-ResNet-v2 without swapping model. It is a generic model where the misclassified data between the training and validation datasets of endemic birds are not interchanged. The other is the Inception-ResNet-v2 swapping model in which the misclassified data are swapped between the training and validation datasets of endemic birds. In this model, bird data is split into 80% for training and 20% for validation. Thereafter, validation data are tested from the well-trained model. If the validation test yielded more than 15 misclassified images, then the number of misclassified bird images are interchanged with the training dataset randomly. Then, the model is retrained again until we get better results. Furthermore, fivefold cross-validation is performed to evaluate the stability of the model. A comparison of the performance of the two models with the various datasets is presented in Table 1.

TABLE 1. **Performance Comparison Between Models with and Without Swapping of the Misclassified Data with the Training and Validation Datasets.**

**Without swapping model			**With swapping model		
TA (%)	VA (%)	EA (%)	TA (%)	VA (%)	EA (%)
100	97.47	97.11	100	99.63	98.42
VEI	CCI	MCI	VEI	CCI	MCI
3480	3392	88	3480	3467	13
TEI	CCI	MCI	TEI	CCI	MCI
760	738	22	760	748	12

**TA: training accuracy, VA: validation accuracy, EA: test accuracy, VEI: validation images, CCI: correctly classified images, MCI: misclassified images, TEI: total test images.

TABLE 2. **Performance Before and After Swapping the Misclassified Data with the Training and Validation Datasets.**

Fivefold	Accuracy (%)	
	Without swapping model	With swapping model
Fold 1	97.11	98.42
Fold 2	96.84	98.29
Fold 3	97.11	98.42
Fold 4	97.11	98.42
Fold 5	97.11	98.42
Average	97.06	98.39

In multistage model validation particularly, the performance of the Inception-ResNet-v2 with swapping model was considerably higher than that of the model without swapping, as indicated by the validation and test accuracies. For instance, the Inception-ResNet-v2 without swapping model achieved a validation accuracy of 97.47% from 3,480 images (3,392 bird images were correctly classified and 88 were misclassified) and a test accuracy of 97.11% from 760 images (738 bird images were correctly classified and 22 were misclassified). The Inception-ResNet-v2 with swapping model achieved a validation accuracy of 99.63% from 3,480 images (3467 bird images were correctly classified and 13 were misclassified) and a test accuracy of 98.42% from 760 images (748 bird images were correctly classified and 12 were misclassified). Additionally, fivefold cross-validation was performed for both models. Table 2 presents the fivefold cross-validation results for both models. The Inception-ResNet-v2 without swapping model achieved an average accuracy of 97.06%, whereas the Inception-ResNet-v2 with swapping model achieved an average accuracy of 98.39%. This indicates that the backbone Inception-ResNet-v2 with swapping model provides a clear benchmark for the classification and identification of endemic birds.

C. PERFORMANCE EVALUATION

The performance of the trained models in identifying individual bird species was evaluated using three standard metrics: precision, recall, and F1-score.

$$Precision = \frac{TP}{TP + FP} \tag{3}$$

$$Recall = \frac{TP}{TP + FN} \tag{4}$$

$$F1 - score = 2 * \frac{Recall * Precision}{Recall + Precision} \tag{5}$$

- TP is the true positive, indicating the number of birds correctly detected as endemic birds.
- TN is the true negative, indicating the number of birds correctly detected as nonendemic birds.
- FP is the false positive, indicating the number of birds incorrectly detected as endemic birds.
- FN is the false negative, indicating the number of ground truth birds undetected by the predictive system.

Thus, precision quantifies the number of bird predictions that actually belong to the 29 endemic birds, whereas recall represents the probability of correctly classified birds of each class in the dataset. In an ideal model, the precision and recall rates are equal to 1. The F1-score is a quantitative metric that represents the balance between precision and recall. The performance of the model in classifying 29 endemic birds is presented in Table 3. The model achieved an average precision, recall, and F1-score of 98.49%, 97.50%, and 97.90%, respectively.

D. CONFUSION MATRIX

A confusion matrix was applied for quantitative evaluation to verify the prediction accuracy of the model. Most of the misclassified images shared either similar colors or sizes. For instance, Black-necklaced Scimitar-babbler, Mikado Pheasant, Taiwan Hwamei, and Taiwan Shortwing were misclassified to Taiwan Fulvetta, Taiwan Blue-magpie, Taiwan Shortwing, and Taiwan Hwamei, respectively. But Taiwan Barwing was misclassified to other two classes: Rufous-crowned Laughingthrush and Taiwan Shortwing, while Taiwan Scimitar-babbler was misclassified to Black-necklaced Scimitar-babbler and Taiwan Hwamei. However, some images were misclassified due to distance measurement and occlusion of the environment. For example, Steere's Liocichla was misclassified to Collared Bush-robin and White-eared Sibia was misclassified to Taiwan Whistling-thrush. Detailed misclassified distribution is presented in Table 4. In the confusion matrix, each row of the matrix denotes the instances in a predicted class and each column denotes the instances in an actual class of the endemic birds. Yellow highlighted in the table represented the number of misclassified images and the rest indicated the correctly classified images.

Subsequently, the bird images were tested using a mobile app. Fig. 6 shows the interface for the detection of the two newly added endemic birds, namely the Taiwan Thrush (*T. niveiceps*) and Taiwan Shortwing (*B. goodfellowi*).

TABLE 3. Performance Evaluation of 29 Endemic Birds.

Bird Images	Precision (%)	Recall (%)	F1-score (%)
Black-necklaced Scimitar-Babbler	93.75	93.75	93.75
Chestnut-bellied Tit	100.00	100.00	100.00
Collared Bush-Robin	90.48	100.00	95.00
Flamecrest	100.00	100.00	100.00
Mikado Pheasant	100.00	83.33	90.91
Morrison's Fulvetta/Gray-cheekeed Fulvetta	100.00	100.00	100.00
Rufous-crowned Laughingthrush	98.25	100.00	99.12
Rusty Laughingthrush	94.44	100.00	97.14
Styan's Bulbul	100.00	87.50	93.33
Steere's Liocichla	100.00	86.67	92.86
Swinhoe's Pheasant	100.00	100.00	100.00
Taiwan Bamboo-Partridge	100.00	100.00	100.00
Taiwan Barbet	100.00	100.00	100.00
Taiwan Barwing	100.00	100.00	100.00
Taiwan Blue-Magpie	91.67	100.00	95.65
Taiwan Bush Warbler	100.00	100.00	100.00
Taiwan Cupwing	100.00	100.00	100.00
Taiwan Fulvetta	100.00	100.00	100.00
Taiwan Hwamei	96.30	96.30	96.30
Taiwan Partridge	100.00	100.00	100.00
Taiwan Rosefinch	100.00	100.00	100.00
Taiwan Scimitar-Babbler	100.00	89.47	94.44
Taiwan Shortwing	96.36	98.15	97.25
Taiwan Thrush/Taiwan Island Thrush	98.33	100.00	99.16
Taiwan Whistling-Thrush	96.55	100.00	98.25
Taiwan Yuhina	100.00	100.00	100.00
White-eared Sibia	100.00	92.31	96.00
White-whiskered Laughingthrush	100.00	100.00	100.00
Yellow Tit	100.00	100.00	100.00
Average	98.49	97.50	97.90

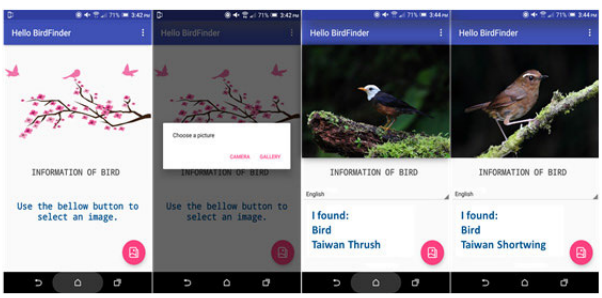

FIGURE 6. Two newly added birds' endemic to Taiwan.

VI. IMPACT AND SIGNIFICANCES OF ENDEMIC BIRDS

Taiwan is a small island of 36,000 km^2, but it has a large number of avian species, including migrants and vagrants. More than 624 species have been recorded, including 29 endemic bird species and more than 55 endemic subspecies. Taiwan's coastal areas and outlying islands such as Penghu, Kinmen, Matsu, and Orchid Island, are major corridors on the EAAF, through which many birds migrate between their breeding and nonbreeding seasons. They migrate north to as far as Siberia during the summer season and south to as far as Indonesia, Australia, and New Zealand during the winter season. This migration of birds causes species habitat hybridization and biodiversity loss. Thus, to ensure the continued existence of endemic birds and alleviate a major source of species destruction of species, habitat conservation is essential and of primary importance for the conservation of prolific biological resources. For instance, the Styan's Bulbul (*Pycnonotus taivanus*), which is also known as the Formosan Black Head Bulbul or Taiwan Black Head Bulbul, is an endemic species of bulbul in the Pycnonotidae family. This species is found in eastern and southern Taiwan, and it is listed as a species that is in danger of extinction. It is in decline owing to habitat destruction and hybridization with the closely related Chinese or Light-Vented Bulbul (*P. sinensis*), a species of bird also in the Pycnonotidae family, which is mainly found in central and southern China, northern Vietnam, and Taiwan. The Styan's Bulbul habitat environment and body plumage are similar to those of the Chinese Bulbul; however, their head features differ. The Styan's Bulbul has a completely black crown with white feathers around its eyes. The cheeks, ears, and throat are gray and white, and it has a prominent orange-red spot at the corner of the lower mouth and a thick black jawline extending rearward from the corners of the mouth. The back of the Styan's Bulbul is dark brown in color with a bit of olive yellow on the wings; their upper chest is grayish brown, and their abdomen is grayish white. The tarsals and toes are black. The Chinese Bulbul has a large white patch of hindcrown covering the nape and sides of its black head. The cheeks are black, and only the back of the eyes has a small white spot. Styan's Bulbuls are spotted in Taroko National Park, Kenting National Park, and Shoushan National Natural Park. They mostly feed on seeds, fruits, flowers, and insects. Fig. 7(a) shows the Styan's Bulbul, and Fig. 7(b) shows the Chinese Bulbul.

(a) (b)

FIGURE 7. (a) Styan's Bulbul (P. taivanus). (b) Chinese bulbul (P. sinensis).

According to the georeferenced locality records of BirdLife International, Taiwan is mapped as an Endemic Bird Area (EBA) because it contains avian habitats of restricted range that must be conserved. Geographically, EBAs are often distributed in islands or mountain ranges that are generally located in the tropics and subtropics. The distribution of the 29 endemic bird species in the national parks

TABLE 4. **Confusion Matrix of the Classification of 29 Endemic Bird Species.**

	1	2	3	4	5	6	7	8	9	10	11	12	13	14	15	16	17	18	19	20	21	22	23	24	25	26	27	28	29
1*	**15**	0	0	0	0	0	0	1	0	0	0	0	0	0	0	0	0	0	0	0	0	0	0	0	0	0	0	0	0
2*	0	**78**	0	0	0	0	0	0	0	0	0	0	0	0	0	0	0	0	0	0	0	0	0	0	0	0	0	0	0
3*	0	0	**19**	0	0	0	0	0	0	0	0	0	0	0	0	0	0	0	0	0	0	0	0	0	0	0	0	0	0
4*	0	0	0	**14**	0	0	0	0	0	0	0	0	0	0	0	0	0	0	0	0	0	0	0	0	0	0	0	0	0
5*	0	0	0	0	**10**	0	0	0	0	0	0	0	0	0	2	0	0	0	0	0	0	0	0	0	0	0	0	0	0
6*	0	0	0	0	0	**15**	0	0	0	0	0	0	0	0	0	0	0	0	0	0	0	0	0	0	0	0	0	0	0
7*	0	0	0	0	0	0	**55**	0	0	0	0	0	0	0	0	0	0	0	0	0	0	0	0	0	0	0	0	0	0
8*	0	0	0	0	0	0	0	**17**	0	0	0	0	0	0	0	0	0	0	0	0	0	0	0	0	0	0	0	0	0
9*	0	0	0	0	0	0	1	0	**14**	0	0	0	0	0	0	0	0	0	0	0	0	0	1	0	0	0	0	0	0
10*	0	0	2	0	0	0	0	0	0	**13**	0	0	0	0	0	0	0	0	0	0	0	0	0	0	0	0	0	0	0
11*	0	0	0	0	0	0	0	0	0	0	**14**	0	0	0	0	0	0	0	0	0	0	0	0	0	0	0	0	0	0
12*	0	0	0	0	0	0	0	0	0	0	0	**29**	0	0	0	0	0	0	0	0	0	0	0	0	0	0	0	0	0
13*	0	0	0	0	0	0	0	0	0	0	0	0	**12**	0	0	0	0	0	0	0	0	0	0	0	0	0	0	0	0
14*	0	0	0	0	0	0	0	0	0	0	0	0	0	**40**	0	0	0	0	0	0	0	0	0	0	0	0	0	0	0
15*	0	0	0	0	0	0	0	0	0	0	0	0	0	0	**22**	0	0	0	0	0	0	0	0	0	0	0	0	0	0
16*	0	0	0	0	0	0	0	0	0	0	0	0	0	0	0	**14**	0	0	0	0	0	0	0	0	0	0	0	0	0
17*	0	0	0	0	0	0	0	0	0	0	0	0	0	0	0	0	**18**	0	0	0	0	0	0	0	0	0	0	0	0
18*	0	0	0	0	0	0	0	0	0	0	0	0	0	0	0	0	0	**14**	0	0	0	0	0	0	0	0	0	0	0
19*	0	0	0	0	0	0	0	0	0	0	0	0	0	0	0	0	0	0	**26**	0	0	0	1	0	0	0	0	0	0
20*	0	0	0	0	0	0	0	0	0	0	0	0	0	0	0	0	0	0	0	**12**	0	0	0	0	0	0	0	0	0
21*	0	0	0	0	0	0	0	0	0	0	0	0	0	0	0	0	0	0	0	0	**32**	0	0		0	0	0	0	0
22*	1	0	0	0	0	0	0	0	0	0	0	0	0	0	0	0	0	0	1	0	0	**17**	0	0	0	0	0	0	0
23*	0	0	0	0	0	0	0	0	0	0	0	0	0	0	0	0	0	0	1	0	0	0	**53**	0	0	0	0	0	0
24*	0	0	0	0	0	0	0	0	0	0	0	0	0	0	0	0	0	0	0	0	0	0	0	**59**	0	0	0	0	0
25*	0	0	0	0	0	0	0	0	0	0	0	0	0	0	0	0	0	0	0	0	0	0	0	0	**28**	0	0	0	0
26*	0	0	0	0	0	0	0	0	0	0	0	0	0	0	0	0	0	0	0	0	0	0	0	0	0	**18**	0	0	0
27*	0	0	0	0	0	0	0	0	0	0	0	0	0	0	0	0	0	0	0	0	0	0	0	0	1	0	**12**	0	0
28*	0	0	0	0	0	0	0	0	0	0	0	0	0	0	0	0	0	0	0	0	0	0	0	0	0	0	0	**36**	0
29*	0	0	0	0	0	0	0	0	0	0	0	0	0	0	0	0	0	0	0	0	0	0	0	0	0	0	0	0	**42**

*1-Black-necklaced Scimitar-Babbler, *2-Chestnut-bellied Tit, *3-Collared Bush-Robin, *4-Flamecrest, *5-Mikado Pheasant, *6-Morrison's Fulvetta/Gray-cheekeed Fulvetta, *7-Rufous-crowned Laughing thrush, *8-Rusty Laughing thrush, *9-Styan's Bulbul, *10-Steere's Liocichla, *11-Swinhoe's Pheasant, *12-Taiwan Bamboo-Partridge, *13-Taiwan Barbet, *14-Taiwan Barwing, *15-Taiwan Blue Magpie, *16-Taiwan Bush Warbler, *17-Taiwan Cupwing, *18-Taiwan Fulvetta, *19-Taiwan Hwamei, *20-Taiwan Partridge, *21-Taiwan Rosefinch, *22-Taiwan Scimitar-Babbler, *23-Taiwan Shortwing, *24-Taiwan Thrush/Taiwan Island Thrush, *25-Taiwan Whistling-Thrush, *26-Taiwan Yuhina, *27-White-eared Sibia, *28-White-whiskered Laughing thrush, *29-Yellow Tit.

(Yangmingshan National Park, Shei-pa National Park, Taroko National Park, Yushan National Park, Kenting National Park, and Shoushan National Natural Park) [34] of Taiwan are shown in Fig. 8(a). Fig. 8(b) and 8(c) show the distribution of the two newly added endemic birds, Taiwan Thrush (*T. niveiceps*) and Taiwan Shortwing (*B. goodfellowi*) of Taiwan, respectively.

Most birds have quite special characteristics from the perspective of ecosystem services. Additionally, they have inspired humans for centuries by helping us understand evolution through natural selection, providing ideas that have helped facilitate air travel, and indicating the need to respond quickly to preserve the health of the planet. The Taiwan Barbet (*Psilopogon nuchalis*), which is also known as the Formosan Barbet, is an endemic species of bird in the Megalaimidae family. This unique bird is an endangered and protected species of Taiwan. The Formosan Barbet has a mostly emerald-green body and iridescent face with five-color feathers. The five colors are exactly the same as the colors of the five interlaced Olympic rings, which represent the five continents of the world (Europe, Asia, Africa, America, and Oceania): blue, yellow, black, red, and green. Locally, the Taiwan Barbet is also known as "Wuseniao." The name "Wuse" refers to the five colors on their feathers. The head is mostly blue, the forehead and throat are yellow, the upper part of the ear and the thick mouth part are black with many black tassels on their beak, the front of the eyes and the front of the neck have a bit of red, and the entire body is covered in bright green colorful feathers. The length of the bird is 20–23 cm. They are mostly distributed in woodlands and broadleaf forests, and their preferred habitats are hot and humid conditions. This five-color bird is a primary cavity

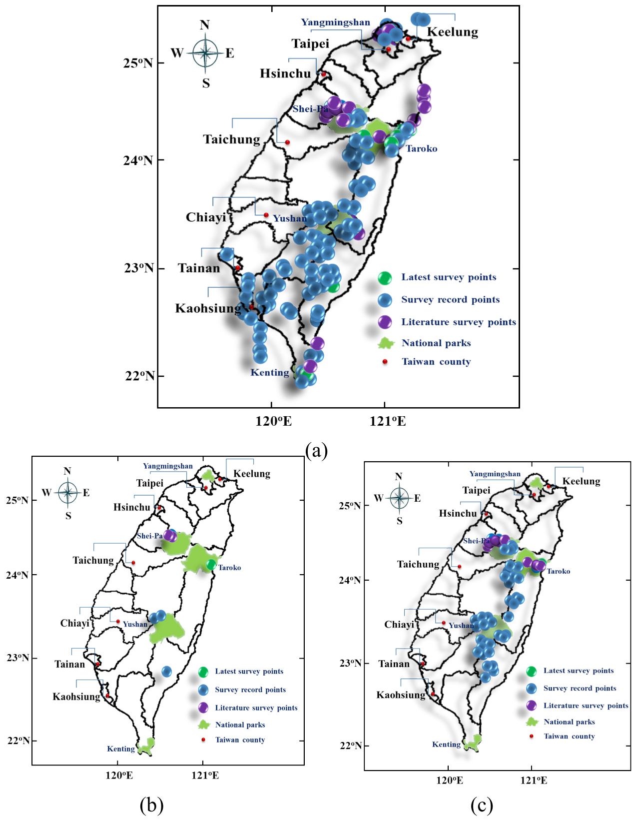

FIGURE 8. **Endemic bird distribution of Taiwan (Record of the most recent survey: Taroko National Park 11-23-2019). (a) 29 endemic bird species distribution in the national parks. (b) Taiwan Thrush (*Turdus niveiceps*) distribution in the national parks. (c) Taiwan Shortwing (*Brachypteryx goodfellowi*) distribution in the national parks.**

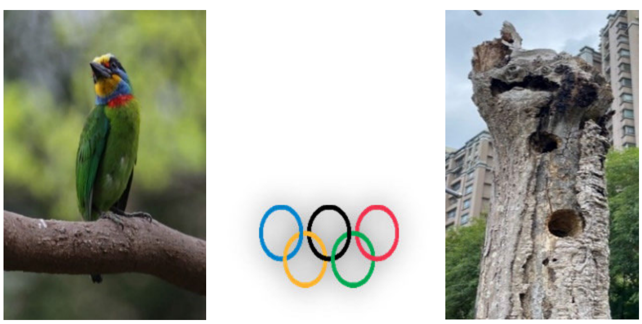

(a) (b) (c)

FIGURE 9. **(a) Taiwan Barbet with five-color feathers. (b) Five colors of Olympic game rings. (c) Nest cavity of Taiwan Barbet.**

nester in dead trees; the nests are usually 5 cm in diameter and 20–25 cm in depth. They prefer trees with a large diameter of dead wood to easily build their nests. Fig. 9(a), 9(b), and 9(c) show the Taiwan Barbet with five-color feathers, the five-color interlocking rings of the Olympic games, and the nest cavity of the Taiwan Barbet, respectively.

The Taiwan Barbet is found in Yangmingshan National Park, Taroko National Park, Shei-pa National Park, Yushan National Park, Kenting National Park, and Shoushan National Natural Park. The Taiwan Barbet mostly feeds on fruits, which constitute a large part of their diet. Thus, birds provide regeneration and resilience to ecosystems to sustain their biodiversity. Thus, it is essential to identify endemic birds that are prone to invasion by ecologically similar species that may eventually cause niche domination or the extirpation of species already existing on the island.

VII. CONCLUSION

In this study, we developed a new transfer learning method that has the inherent ability to transfer perceived knowledge from endemic birds; this knowledge was then used for solving the problem of classifying two newly identified endemic birds. To validate our proposed model, we compared its performance with that of four different state-of-the-art deep learning classification models with transfer learning. Furthermore, the designed model was reinforced with multistage model validation by swapping misclassified data between the training and validation datasets to achieve better results in the detection and classification of birds. Our model achieved an accuracy of 98.39% in the classification of 29 endemic bird species and an accuracy of 100% in the detection of birds among different object categories. Moreover, the model achieved a precision, recall, and F1-score of 98.49%, 97.50%, and 97.90%, respectively, in the classification of bird species endemic to Taiwan. The developed model can help in the conservation of species by identifying the distribution of species and monitoring adverse environmental effects on bird ecology and their habitat. Moreover, it can help provide a model to forecast a pathway for migratory birds.

In the future, we aim to develop a web crawler system that can automatically harvest and identify global endemic bird species to determine threatened and rare species richness.

REFERENCES

[1] B. Reyers and E. R. Selig, "Global targets that reveal the social–ecological interdependencies of sustainable development," *Nature Ecol. Evol.*, vol. 4, no. 8, pp. 1011–1019, Jul. 2020.

[2] F. He and S. P. Hubbell, "Species—Area relationships always overestimate extinction rates from habitat loss," *Nature*, vol. 473, no. 7347, pp. 368–371, May 2011.

[3] A. Perrin, A. Khimoun, B. Faivre, A. Ollivier, N. de Pracontal, F. Théron, M. Loubon, G. Leblond, O. Duron, and S. Garnier, "Habitat fragmentation differentially shapes neutral and immune gene variation in a tropical bird species," *Heredity*, vol. 126, no. 1, pp. 148–162, Sep. 2020.

[4] D. A. Wilkinson, J. C. Marshall, N. P. French, and D. T. S. Hayman, "Habitat fragmentation, biodiversity loss and the risk of novel infectious disease emergence," *J. Roy. Soc. Interface*, vol. 15, pp. 1–10, Dec. 2018.

[5] G. Strona and K. D. Lafferty, "Environmental change makes robust ecological networks fragile," *Nature Commun.*, vol. 7, no. 1, pp. 1–7, Aug. 2016.

[6] M. G. Betts, C. Wolf, M. Pfeifer, C. Banks-Leite, V. Arroyo-Rodríguez, D. B. Ribeiro, J. Barlow, F. Eigenbrod, D. Faria, R. J. Fletcher, and A. S. Hadley, "Extinction filters mediate the global effects of habitat fragmentation on animals," *Science*, vol. 366, pp. 1236–1239, Dec. 2019.

[7] T. Telenský, P. Klvaňa, M. Jelínek, J. Cepák, and J. Reif, "The influence of climate variability on demographic rates of avian afro-palearctic migrants," *Sci. Rep.*, vol. 10, no. 1, pp. 1–11, Oct. 2020.

[8] J. T. Ibarra and K. Martin, "Biotic homogenization: Loss of avian functional richness and habitat specialists in disturbed andean temperate forests," *Biol. Conservation*, vol. 192, pp. 418–427, Dec. 2015.

[9] J. L. Blanchard, "A rewired food web," *Nature*, vol. 527, no. 7577, pp. 173–174, Nov. 2015.

[10] R. Inger, E. Per, D. T. C. Cox, and K. J. Gaston, "Key role in ecosystem functioning of scavengers reliant on a single common species," *Sci. Rep.*, vol. 6, no. 1, pp. 1–5, Jul. 2016.

[11] R. S. C. Cooke, F. Eigenbrod, and A. E. Bates, "Projected losses of global mammal and bird ecological strategies," *Nature Commun.*, vol. 10, no. 1, pp. 1–8, May 2019.

[12] A. A. A. Bovo, K. M. P. M. B. Ferraz, M. Magioli, E. R. Alexandrino, É. Hasui, M. C. Ribeiro, and J. A. Tobias, "Habitat fragmentation narrows the distribution of avian functional traits associated with seed dispersal in tropical forest," *Perspect. Ecol. Conservation*, vol. 16, no. 2, pp. 90–96, Apr. 2018.

[13] (2017). *BirdLife International. IUCN Red List for Birds. Version 2017.1*. BirdLife International. [Online]. Available: http://www.birdlife.org

[14] *Data Zone. State of the World's Birds: 2020 Annual Update*. Accessed: May 25, 2021. [Online]. Available: http://datazone.birdlife.org/sowb/state

[15] R. G. Pearson, "Reasons to conserve nature," *Trends Ecol. Evol.*, vol. 31, no. 5, pp. 366–371, May 2016.

[16] Birdlife. 2020. *East Asia/Australasia Flyway*. [Online]. Available: https://www.birdlife.org/sites/default/files/attachments/8_East_Asia_Australasia_Factsheet.pdf

[17] P.-F. Lee, T.-S. Ding, F.-H. Hsu, and S. Geng, "Breeding bird species richness in Taiwan: Distribution on gradients of elevation, primary productivity and urbanization," *J. Biogeography*, vol. 31, no. 2, pp. 307–314, Feb. 2004.

[18] *Clements Checklist*. Accessed: May 25, 2021. [Online]. Available: https://www.birds.cornell.edu/clementschecklist/download/

[19] J. Li, A. C. Hughes, and D. Dudgeon, "Mapping wader biodiversity along the East Asian—Australasian flyway," *PLoS ONE*, vol. 14., no. 1, pp. 1–26, Jan. 2019.

[20] M. Somveille, M. Wikelski, R. M. Beyer, A. S. L. Rodrigues, A. Manica, and W. Jetz, "Simulation-based reconstruction of global bird migration over the past 50,000 years," *Nature Commun.*, vol. 11, no. 1, pp. 1–9, Feb. 2020.

[21] Y. Huang and H. Basanta, "Bird image retrieval and recognition using a deep learning platform," *IEEE Access*, vol. 7, pp. 66980–66989, 2019.

[22] J. Wang, Y. Chen, W. Feng, H. Yu, M. Huang, and Q. Yang, "Transfer learning with dynamic distribution adaptation," *ACM Trans. Intell. Syst. Technol.*, vol. 11, no. 1, pp. 1–25, Feb. 2020.

[23] H. Jiang, K. Wang, Y. Wang, M. Gao, and Y. Zhang, "Energy big data: A survey," *IEEE Access*, vol. 4, pp. 3844–3861, 2016.

[24] R. Liu, Y. Shi, C. Jia, and M. Jia, "A survey of sentiment analysis based on transfer learning," *IEEE Access*, vol. 7, pp. 85401–85412, 2019.

[25] S. J. Pan and Q. Yang, "Survey on transfer learning," *IEEE Trans. Knowl. Data Eng.*, vol. 22, no. 10, pp. 1345–1359, Oct. 2010.

[26] L. Shao, F. Zhu, and X. Li, "Transfer learning for visual categorization: A survey," *IEEE Trans. Neural Netw. Learn. Syst.*, vol. 26, no. 5, pp. 1019–1034, May 2015.

[27] C. Szegedy, S. Ioffe, V. Vanhoucke, and A. Alemi, "Inception-v4, inception-ResNet and the impact of residual connections on learning," 2016, *arXiv:1602.07261*. [Online]. Available: http://arxiv.org/abs/1602.07261

[28] C. Szegedy, W. Liu, Y. Jia, P. Sermanet, S. Reed, D. Anguelov, D. Erhan, V. Vanhoucke, and A. Rabinovich, "Going deeper with convolutions," 2014, *arXiv:1409.4842*. [Online]. Available: http://arxiv.org/abs/1409.4842

[29] K. He, X. Zhang, S. Ren, and J. Sun, "Deep residual learning for image recognition," 2015, *arXiv:1512.03385*. [Online]. Available: http://arxiv.org/abs/1512.03385

[30] L. Jiao, F. Zhang, F. Liu, S. Yang, L. Li, Z. Feng, and R. Qu, "A survey of deep learning-based object detection," *IEEE Access*, vol. 7, pp. 128837–128868, 2019.

[31] W. G. Hatcher and W. Yu, "A survey of deep learning: Platforms, applications and emerging research trends," *IEEE Access*, vol. 6, pp. 24411–24432, 2018.

[32] F. Chollet, "Xception: Deep learning with depthwise separable convolutions," 2016, *arXiv:1610.02357*. [Online]. Available: http://arxiv.org/abs/1610.02357

[33] A. G. Howard, M. Zhu, B. Chen, D. Kalenichenko, W. Wang, T. Weyand, M. Andreetto, and H. Adam, "MobileNets: Efficient convolutional neural networks for mobile vision applications," 2017, *arXiv:1704.04861*. [Online]. Available: http://arxiv.org/abs/1704.04861

[34] *National Parks of Taiwan Biodiversity Database*. Accessed: May 25, 2021. [Online]. Available: https://npgis.cpami.gov.tw/newpublic

YO-PING HUANG (Fellow, IEEE) received the Ph.D. degree in electrical engineering from Texas Tech University, Lubbock, TX, USA. He is currently the President of the National Penghu University of Science and Technology, Penghu, Taiwan. He is also the Chair Professor with the Department of Electrical Engineering, National Taipei University of Technology, Taipei, Taiwan, where he worked as the Secretary General. He was a Professor and the Dean of Research and Development, the Dean of the College of Electrical Engineering and Computer Science, and the Department Chair with Tatung University, Taipei. His current research interests include fuzzy systems design and modeling, deep learning modeling, intelligent control, medical data mining, and rehabilitation systems design.

He serves as the IEEE SMCS BoG, the Chair of the IEEE SMCS Technical Committee on Intelligent Transportation Systems, and the Chair of the Taiwan SIGSPATIAL ACM Chapter. He was the President of the Taiwan Association of Systems Science and Engineering, the Chair of the IEEE SMCS Taipei Chapter, the Chair of the IEEE CIS Taipei Chapter, and the CEO of the Joint Commission of Technological and Vocational College Admission Committee, Taiwan. He is an IET Fellow, CACS Fellow, and an International Association of Grey System and an Uncertain Analysis Fellow.

HAOBIJAM BASANTA received the Master of Science degree in computer application (MCA) from the University of Jamia Millia Islamia, Delhi, India, and the Ph.D. degree in electrical engineering and computer science from the National Taipei University of Technology, Taipei, Taiwan. He is currently holds a postdoctoral position with the National Taipei University of Technology. His current research interests include artificial intelligence (AI), the Internet of Things (IoT) for elderly healthcare systems, big data analytics, deep learning, and image processing.